

438-10-223 203

Copy  
RM L54H17

NACA RM L54H17

7573

0143555  
TECH LIBRARY KAFB, NM

**NACA**

# RESEARCH MEMORANDUM

FREE-FLIGHT MEASUREMENTS OF THE ROLLING EFFECTIVENESS  
AND OPERATING CHARACTERISTICS OF A BELLOWS-ACTUATED  
SPLIT-FLAP AILERON ON A 60° DELTA WING AT  
MACH NUMBERS BETWEEN 0.8 AND 1.8

By Eugene D. Schult

Langley Aeronautical Laboratory  
Langley Field, Va.

~~This document contains information affecting the national defense of the United States within the meaning of the espionage laws, Title 18, U.S.C., Sec. 793 and 794, and the transmission or revelation of its contents in any manner to an unauthorized person is prohibited by law.~~

**NATIONAL ADVISORY COMMITTEE  
FOR AERONAUTICS**

WASHINGTON

October 18, 1954

Classification cancelled (or changed to Unclassified)

By Authority of 1st ASST. TECH. LAB. ANNOUNCEMENT #1  
(OFFICER AUTHORIZED TO CHANGE)

By 14 NOV 58

SAVP  
GRADE OF OFFICER MAKING CHANGE

28 MAR 61  
DATE



## NATIONAL ADVISORY COMMITTEE FOR AERONAUTICS

## RESEARCH MEMORANDUM

## FREE-FLIGHT MEASUREMENTS OF THE ROLLING EFFECTIVENESS

## AND OPERATING CHARACTERISTICS OF A BELLOWS-ACTUATED

## SPLIT-FLAP AILERON ON A 60° DELTA WING AT

## MACH NUMBERS BETWEEN 0.8 AND 1.8

By Eugene D. Schult

## SUMMARY

A free-flight investigation has been conducted by the Langley Pilotless Aircraft Research Division in the Mach number range between 0.8 and 1.8 to determine the maximum deflection, the zero-lift rolling effectiveness, and the general operating characteristics of a bellows-actuated aileron control system energized by the pitot (impact) pressure. These tests of a partial-span split-flap aileron on a 60° delta wing indicated that this system affords a promising means for obtaining lateral control at supersonic speeds in that substantial aileron deflections are readily obtained without the aid of an auxiliary servo power supply. Maximum aileron deflections of the order of 20° at a Mach number of 1.8 were measured when using a simple one-cell bellows arrangement, and the deflection generally increased with increasing supersonic Mach number. Higher deflections may be expected with improved bellows design. The maximum rolling effectiveness of the test configuration remained constant at high subsonic speeds; then decreased at supersonic speeds to approximately one-third the subsonic level. No aileron flutter was observed. Suitable methods for regulating the aileron deflection are described.

## INTRODUCTION

One of the problems associated with the design of controls for airplanes and missiles flying at supersonic speeds is that of providing an effective means for overcoming the aerodynamic loads due to control deflection. Because of severe space limitations, the use of massive control elements or a large power-boost system is not always practical, with the result that an increased emphasis has been placed on simplified controls which utilize the energy in the airstream to deflect the control

~~CONFIDENTIAL~~~~11-50-54 11-50-55~~

surface. By this concept it may be possible to eliminate altogether the weight and cost of the servo power supply and storage component.

A proposed lateral control of this type is the bellows-actuated aileron. One possible arrangement (fig. 1) consists of a split-flap aileron which is deflected by means of a pneumatic bellows, using air obtained from a pitot (impact) pressure source. Early investigations with air brakes and landing flaps have shown that large deflections are possible with this system (refs. 1 to 4). So far as is known, the first mention of applying bellows to lateral or other controls where precise control setting is necessary was made in reference 5, which included some preliminary data from the present investigation.

In the present investigation the Langley Pilotless Aircraft Research Division conducted a free-flight test of a simple, bellows-actuated aileron located slightly forward of the trailing edge of a  $60^\circ$  delta wing. This aileron arrangement causes little structural interference with trailing-edge high-lift devices and provides lateral control at low and transonic speeds (refs. 6 and 7); only limited data are available on its effectiveness at supersonic speeds, however. Measurements were made of the maximum aileron deflection and zero-lift rolling effectiveness at Mach numbers between 0.8 and 1.8 and Reynolds numbers between  $4 \times 10^6$  and  $13 \times 10^6$ . Also included are some limited data on aileron hinge moments, aileron response time, bellows effectiveness, and the operating characteristics of a proposed aileron-deflection control system.

#### SYMBOLS

A	aspect ratio, $b^2/S$
S	total wing area, sq ft
b	total wing span, ft
c	chord, ft
$\Lambda$	sweepback angle of wing leading edge, deg
$\delta$	aileron deflection, deg
t	time, sec
V	velocity of model, ft/sec
M	Mach number

R	Reynolds number, based on mean aerodynamic chord of wing
p	rolling velocity of model, radians/sec
$\frac{pb}{2V}$	wing-tip helix angle, radians
P	absolute pressure, lb/sq ft
q	free-stream dynamic pressure, $0.7P_\infty M^2$ , lb/sq ft
P'	pressure coefficient, $\frac{P - P_\infty}{q}$
$y_f$	aileron span, ft
m	moment area of aileron about aileron hinge axis, $c_f y_f/2$ , cu ft
$m_B$	moment area of bellows "footprint" on aileron lower surface about aileron hinge axis, cu ft
$\frac{m_B}{m}$	moment-area ratio indicating effectiveness or mechanical advantage of the bellows
H	aileron hinge moment, positive when tending to reduce the aileron deflection, ft-lb
$C_h$	aileron hinge-moment coefficient (per aileron), $H/2qm$
$C_{h\delta} = \frac{\partial C_h}{\partial \delta}$	
N	number of bellows cells
D	depth of bellows cavity, aileron chords
l	length of air duct, aileron chords
d	inside diameter of air duct, aileron chords
r	radius of control-valve core, aileron chords
w	width of control-valve ports, measured along aileron hinge axis, aileron chords
F	frequency, cycles/sec

- $\phi$  phase-lag angle, deg
- $\beta$  aileron amplitude ratio (ratio of aileron deflection at any given frequency to aileron deflection at zero frequency)
- $k_1, k_2, k_3$  arbitrary constants

Subscripts:

- a atmospheric or static (pressure)
- b base (pressure behind a bluff body, referring to a less-than-atmospheric pressure sink)
- T pitot (impact pressure)
- B bellows
- U upper surface of aileron
- L lower surface of aileron
- f aileron

MODEL

The test vehicle employed in this investigation is illustrated in figure 2 and detailed in figure 3. The delta wings had leading edges swept back  $60^\circ$  and modified hexagonal sections of constant thickness. The ratio of wing thickness to chord varied from 3 percent at the fuselage juncture to a maximum of 9 percent near the tip. A free-to-roll tail assembly stabilized the model longitudinally without introducing rolling moments.

The lateral control system consisted of an essentially free-floating split-flap aileron located on the upper surface of each wing and deflected by means of single-cell bellows (fig. 3(b)). The bellows were ducted to a pitot and base pressure probe through separate control valves (fig. 3(c)). A motor-driven cam programed the control valves so that the ailerons were deflected independently as functions of time. Control valve ① was used to pulse the pressure in bellows ① alternately between the inlet and base pressures. In addition to deflecting the aileron to obtain roll data, this scheme provided an indication of the system time lag over the test Mach number range. Valve ② regulated the deflection of aileron ② in order to provide test data at intermediate deflections. This was

accomplished by varying the flow of air through a static-bleed port so that the bellows pressure could be adjusted to any desired fraction of the inlet pressure. Bench tests of this device indicated that, for a given valve setting, the bellows pressure ratio  $P'_B/P'_T$  was essentially a constant within the range of inlet pressures encountered during the flight tests. The bellows pressure ratio did not vary linearly with valve setting, however, and in the interest of improving the quality of the data it was necessary to modify the cam profile to make the ratio vary linearly with cam rotation and time.

A single probe served as a source of pitot pressure to inflate the bellows and as a reservoir of low base pressures to assist in evacuating the bellows quickly.

#### TEST TECHNIQUE

The flight test was conducted at the Langley Pilotless Aircraft Research Station at Wallops Island, Va. A single-stage booster, consisting of a 6-inch-diameter ABL Deacon rocket motor, accelerated the model at essentially zero lift, yaw, and roll to a maximum Mach number of 1.85 in 3.0 seconds. During this time the control-valve settings were fixed in approximately the positions shown in figure 3(c). After the booster separated from the model, the programming motor was energized; this caused the ailerons to be pulsed and the model to roll alternately to the right and left while decelerating through the test Mach number range.

Measurements were made of the velocity by using continuous-wave Doppler radar and of the rolling velocity by using polarized-wave radio equipment. These data, in conjunction with SCR 584 space radar and radiosonde measurements, permitted an evaluation of the Mach number  $M$  and the wing-tip helix angle  $pb/2V$  as functions of time. Simultaneous telemeter broadcasts provided time histories of the aileron deflections and the bellows pressure, making it possible to determine the maximum aileron deflection  $\delta_{max}$ , the rolling effectiveness of the aileron per degree  $\frac{pb/2V}{\delta}$ , and the aileron hinge-moment coefficient  $C_h$ .

The aileron hinge-moment coefficients, which reflect the hinge moments balanced by bellows (2), were derived by use of the following relation:

$$C_h = \frac{H}{2qm} = \frac{P'_B}{2} \frac{m_B}{m} \quad (1)$$

The moment-area ratio  $\frac{m_B}{m}$  is essentially the mechanical advantage of the bellows and is a constant at a given aileron deflection. Its variation with aileron deflection was determined from a bench test of the configuration by substituting the experimental quantities of hinge moment and bellows pressure into equation (1) and solving for the ratio at the observed aileron deflections. Since the bellows was not attached to the aileron, it was possible to measure only positive hinge moments with this arrangement.

The test Reynolds number, based on the mean aerodynamic chord of the wing, varied between  $4 \times 10^6$  and  $13 \times 10^6$  and is shown plotted against Mach number in figure 4.

#### ACCURACY OF MEASURED DATA

The test results are believed to be accurate within the following limits:

	Subsonic	Supersonic
M . . . . .	$\pm 0.01$	$\pm 0.01$
$p_b/2V$ , radians . . . . .	$\pm 0.003$	$\pm 0.002$
$C_h$ . . . . .	$\pm 0.03$	$\pm 0.02$
$\delta$ , deg . . . . .	$\pm 0.4$	$\pm 0.4$

#### RESULTS AND DISCUSSION

The test results of the present investigation are presented in figures 5 to 9. In figure 5 flight histories of the measured bellows pressure, aileron deflections, and model rolling velocity are plotted against Mach number. The bellows pressure in cell (2) has been reduced to coefficient form and presented as a fraction of the calculated pitot-pressure coefficient. No pressures were measured in cell (1) during the test. The aileron deflection data show that both ailerons floated freely at small deflections; this phenomenon, which was especially noticeable at high subsonic speeds, is attributed to an overbalanced hinge moment condition and will be discussed later. No indications of aileron flutter were observed over the test Mach number range.



### Aileron Rolling Effectiveness

Figure 6 presents the variations with Mach number of the maximum aileron deflection, the rolling effectiveness per degree of aileron deflection, and the maximum rolling effectiveness. The results show that substantial aileron deflections were obtained with a simple, one-cell bellows arrangement and that the maximum deflection generally increased with increasing supersonic Mach number. It will be shown later that larger deflections may be expected if the number of cells is increased. The slightly lower deflection indicated for aileron ① is believed to have been caused by air leakage from valve ① due to construction inaccuracies.

The rolling-effectiveness parameter  $\frac{pb/2V}{\delta}$  was obtained from essentially steady-state values of rolling velocity measured near the maximum deflection of a single aileron. Neglected in this presentation are the small losses in rolling effectiveness (0.5 percent) caused by bearing friction in the free-to-roll tail. The slight deflections of the opposite aileron (fig. 5) have also been neglected, inasmuch as reference 7 has indicated that this aileron may be relatively ineffective at small angles unless a wing slot and deflector plate arrangement is incorporated.

At supersonic speeds the rolling effectiveness of the split-flap aileron used in this investigation is estimated to be approximately the same as that of a conventional sharp-trailing-edge aileron of the same span and chord. In this comparison the measured rolling effectiveness of a full-span trailing-edge aileron on a 60° delta wing (ref. 8) was corrected for differences in aileron span and chord by use of reference 9. The final plot of figure 6 shows that the maximum rolling effectiveness of the present-test configuration remained constant at high subsonic speeds, primarily because of the variations in the maximum aileron deflection. At supersonic speeds the maximum rolling effectiveness decreased to approximately one-third the subsonic level.

### Aileron Hinge Moments

Figure 7 presents the aileron hinge-moment coefficients  $C_h$  and  $C_{h\delta}$  as functions of aileron deflection and Mach number, respectively. These coefficients were derived by use of equation (1) from the aerodynamic hinge moments neutralized by the bellows. The data for the boosted (no-roll) phase of the flight were corrected to essentially steady-state load conditions by taking into account the longitudinal accelerations acting on the aileron. For the coasting (rolling) phase the total error in hinge moment resulting from model deceleration, changes in model rolling velocity, and friction in the aileron hinge was estimated to be less than 2 percent of the maximum hinge moment at a given Mach number and was neglected. A small Mach number correction was made to the data

of figure 7(a) to account for the difference between the actual Mach number and the average Mach number for the cycle; this correction was generally less than 5 percent. The differences between the curves for increasing and decreasing aileron deflections are attributed largely to the differences in the average rolling velocity for the two cases.

The test results at high subsonic speeds are in general agreement with the data of reference 7 for a similar aileron on a thinner wing configuration ( $t/c = 1.5$  to 4.5 percent). An overbalanced hinge moment condition existed at small aileron deflections and caused the ailerons to float as shown in figure 5. The condition, which was more pronounced at subsonic speeds, coincides with the reversed lift and pitching-moment increments observed in other tests of split flaps located forward of the wing trailing edge; the phenomenon occurred when the flow reattached to the wing surface behind the flap (ref. 10).

At supersonic speeds the experimental results are in good agreement with values calculated from simple theory. The calculated values were obtained by use of the following relations:

$$C_h = C_{h_U} + C_{h_L} \quad (2)$$

$$C_{h_U} = \frac{P'_U}{2} \quad (3)$$

$$C_{h_L} = \frac{-P'_b}{2} \left( 1 - \frac{m_B}{m} \right) \quad (4)$$

The pressure coefficients for the upper surface of the aileron  $P'_U$  were calculated from two-dimensional second-order theory. The base pressure coefficient  $P'_b = -1/M^2$  corresponds to a limiting value of negative pressure behind the aileron (ref. 11) and is assumed to act on the lower surface of the aileron not in contact with the bellows.

#### System Time Lag

Since the time required to operate a bellows-actuated aileron may be of interest, measurements were made of the time increments required to deflect the aileron to approximately 90 percent of maximum steady-state aileron deflection and to retract it to approximately zero deflection. The time increments for these two cases were essentially the same and a curve faired through the test points is presented in figure 8. As

a matter of interest, these time intervals are of the same order as those generally obtained with conventional control-pulsing mechanisms.

### Estimation of Aileron Deflection

In appendix A a method is presented for estimating the deflection of a bellows-actuated aileron. These estimates are shown in figure 9 to be in good agreement with experimental values at  $M = 1.76$ . In figure 10 this method is extended to higher Mach numbers in an attempt to determine the variation of the maximum aileron deflection with Mach number and the additional deflection which could be obtained by adding another cell to the bellows. The results indicate that the maximum deflection of the aileron used in the present investigation continues to increase with increasing Mach number and approaches a limiting value of approximately  $30^\circ$  at  $M = 4.0$ . Adding another cell increases this deflection approximately 30 percent. The base pressure behind the aileron is estimated to have little effect on the maximum aileron deflections at these higher Mach numbers.

### Aileron Deflection Control

One difficulty encountered with the present method of regulating the aileron deflection (by regulating the bellows pressure) was that of maintaining precise control over the deflection. As a result, a system incorporating feedback was devised and preliminary bench tests were conducted (appendix B). The results of these tests were encouraging and the system will be used in later research with a pitch control employing a bellows-actuated flap.

### CONCLUSIONS

A free-flight investigation was conducted by the Pilotless Aircraft Research Division in the Mach number range between 0.8 and 1.8 to determine the maximum aileron deflection, the zero-lift rolling effectiveness, and the general control characteristics of a bellows-actuated aileron control system energized by the free-stream pitot pressure. The following conclusions are based on tests of an inboard, partial-span, split-flap aileron located slightly forward of the trailing edge of a  $60^\circ$  delta wing:

1. Maximum aileron deflections of the order of  $20^\circ$  at  $M = 1.8$  were measured with a simple one-cell bellows, and the deflection generally increased with increasing supersonic Mach number. Calculations show that the deflection may be increased further by slight improvements in the bellows design.

2. The maximum rolling effectiveness remained constant at high subsonic speeds and then decreased at supersonic speeds to approximately one-third the subsonic level. At supersonic speeds the effectiveness of this aileron was estimated to be the same as that of a conventional sharp-trailing-edge aileron of the same span and chord.

3. Slightly overbalanced hinge moments were observed at low deflections for this aileron configuration. The phenomenon was more pronounced at subsonic than at supersonic speeds. No indications of aileron flutter were observed over the test Mach number range.

Langley Aeronautical Laboratory,  
National Advisory Committee for Aeronautics,  
Langley Field, Va., July 29, 1954.

## APPENDIX A

## A METHOD FOR ESTIMATING AILERON DEFLECTION

## AT SUPERSONIC SPEEDS

A steady-state deflection of the bellows-actuated aileron occurs when the hinge moment available for balancing (due to the bellows) is equal to the hinge moment required. The hinge moment required is, under static load conditions, essentially equal to the sum of the hinge moments contributed by the aerodynamic pressures acting on both the upper surface of the aileron and the lower surface not in contact with the bellows; that is,

$$C_{h_B} = C_{h_U} + C_{h_L} \quad (A1)$$

where

$$C_{h_B} = \frac{P'_B}{2} \frac{m_B}{m} \quad (A2)$$

$$C_{h_U} = \frac{P'_U}{2} \quad (A3)$$

$$C_{h_L} = \frac{-P'_b}{2} \left( 1 - \frac{m_B}{m} \right) \quad (A4)$$

The moment-area ratio or bellows effectiveness parameter  $\frac{m_B}{m}$  is a function of the aileron deflection and can be either estimated or determined experimentally from bench tests of a given bellows configuration. An estimation of the ratio for cell-type bellows acting on ailerons with rectangular plan forms is given by the equation

$$\frac{m_B}{m} = k_1 k_2 k_3 \quad (A5)$$

where

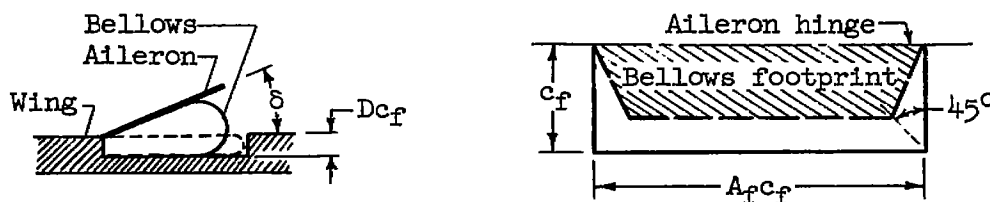
$$k_1 = \left[ \frac{1}{1 + \frac{\pi}{2} \left( \tan \frac{\delta}{2N} \right) \left( 1 + \frac{\delta}{180N} \right)} \right]^2 \quad (A6)$$

The term  $k_1$  is, for  $N$  cells, the calculated moment-area ratio for an infinitely thin, nonstretching, flexible bellows maintained by internal pressure in contact with an infinitely long aileron. The corrections to account for the losses in bellows effectiveness associated with finite bellows thicknesses (cavity depth  $D$ ) and length-to-chord ratios  $A_f$  are reflected in terms  $k_2$  and  $k_3$ , respectively. These corrections are:

$$k_2 = \left[ 1 - \frac{D}{2N} \left( 1 + \frac{\pi\delta}{180N} \right) \right]^2 \quad (A7)$$

$$k_3 = 1 - \frac{4}{3A_f} \left( 1 - \sqrt{k_1 k_2} \right) \quad (A_f \gtrsim 2) \quad (A8)$$

The following illustration shows the assumed bellows "footprint" used in deriving equations (A6) to (A8).



A comparison of the calculated ratio  $\frac{m_B}{m}$  with values experimentally derived for the present-test configuration is shown in figure 11(a). The experimental values were slightly lower at the higher aileron deflections. Figure 11(b) illustrates the fact that the effectiveness of the bellows may be improved significantly by increasing the number of cells.

Using the calculated moment-area ratio (eq. (A5)), the aileron deflections of the test configuration were estimated for  $M = 1.76$  by means of equations (A1) to (A4). The pressure coefficient  $P'_U$  was calculated from two-dimensional second-order theory, and  $P'_b$ , the limiting negative pressure coefficient behind the aileron ( $P'_b = -1/M^2$ ), was obtained from reference 11. The results are presented in figure 9 and show good agreement with experimental values.

## APPENDIX B

## AILERON DEFLECTION CONTROL

In the test configuration the aileron deflection was regulated by proportioning the pressure in the bellows between the static and the pitot pressures (fig. 5). This simple method is generally not suitable for maintaining precise control over the aileron, especially when the maximum deflection varies with Mach number and when nonlinear hinge moments are likely to occur. One method of obtaining precise aileron deflection control is to provide the system with feedback (fig. 12), so that any variations from the desired deflection, which may result from an increase or decrease in hinge moments, will be compensated for by the maximum positive or negative pressures available.

A mock-up of a bellows-actuated aileron based on the system shown in figure 12(a) is illustrated in figure 13, and results of static response tests are presented in figure 14. The aileron hinge-moment loading was simulated for  $M = 1.9$  and the inlet pressure used was the pitot pressure at this Mach number. The results show that, with full pitot pressure available ( $P'/P'_T = 1.0$ ), the output is linear with input until the maximum aileron deflection at this Mach number is approached ( $21^\circ$ ). The difference between the experimental and perfect response curves was caused largely by air leakage resulting from valve construction inaccuracies. A good indication of the control "stiffness" may be gained by comparing the curves for  $P'/P'_T = 1.0$  and  $P'/P'_T = 0.7$ ; here a 30-percent reduction in the available pressure for the same aileron loading is analogous to approximately a 40-percent increase in aileron hinge moment when  $P'/P'_T = 1.0$ . Similarly, a 70-percent reduction in the available pressure for the same loading is analogous to a 300-percent increase in hinge moment.

Some limited data on the frequency-response characteristics of this configuration are presented in figure 15. These tests were of an exploratory nature, not intended to determine an optimum configuration, but to illustrate the effects of variations in several design parameters on the control response. Due to the method of applying the load, some friction damping was introduced which may have altered the general shape of the curves somewhat; this should not, however, impair the usefulness of the data. In the presentation the amplitude ratio is defined as the ratio of the aileron deflection at any given frequency to the aileron deflection at zero frequency.

The results show that an increase in input amplitude from  $6^\circ$  to  $16^\circ$  (reflecting a 60-percent increase in bellows volume) or changes in the available pressure or duct dimensions produced only slight changes in the response of the configuration. The greatest improvement in the frequency response was obtained by increasing the valve port width  $w$ .

## REFERENCES

1. Jacobs, H. H., and Bayless, R. L.: Rolling and Yawing Moment Tests of 1/10 Scale Model Boeing P-26 With L.P.R. Corp. Bellows Flaps, Lift Spoilers and Skewed Ailerons. Five-Foot Wind Tunnel Test No. 120. Air Corps Tech. Rep. Ser. No. 4043, Materiel Div., War Dept., Jan. 22, 1935.
2. Warden, R., and Cheers, F.: Notes on Bellows Flaps. Rep. No. Ae.1911, British N.P.L. (Rep. No. 5582, A.R.C.), Jan. 15, 1942.
3. Anon.: Beaufighter I., R.2057. (2-Hercules III.) Tests With Split Trailing Edge Air Brakes. 13th Pt. of Rep. No. A. & A.E.E./758 (British), June 8, 1942.
4. David, F. W., and Ring, I. H.: Investigations on Bellows Flaps. Rep. ACA-21, Australian Council for Aeronautics, Feb. 1946.
5. Curfman, Howard J., Jr., Strass, H. Kurt, and Crane, Harold L.: Investigations Toward Simplification of Missile Control Systems. NACA RM L53I21a, 1953.
6. Wiley, Harleth G., and Solomon, Martin: A Wind-Tunnel Investigation at Low Speeds of the Aerodynamic Characteristics of Various Spoiler Configurations on a Thin 60° Delta Wing. NACA RM L52J13, 1952.
7. Wiley, Harleth G., and Taylor, Robert T.: Investigation at Transonic Speeds of the Lateral-Control and Hinge-Moment Characteristics of a Flap-Type Spoiler Aileron on a 60° Delta Wing. NACA RM L53J05, 1954.
8. Sandahl, Carl A.: Free-Flight Investigation of the Rolling Effectiveness of Several Delta Wing-Aileron Configurations at Transonic and Supersonic Speeds. NACA RM L8D16, 1948.
9. Tucker, Warren A., and Nelson, Robert L.: Theoretical Characteristics in Supersonic Flow of Two Types of Control Surfaces on Triangular Wings. NACA Rep. 939, 1949. (Supersedes NACA TN's 1600, 1601, and 1660.)
10. Holford, J. F., and Leathers, J. W.: Low Speed Tunnel Tests of Some Split Flap Arrangements on a 48° Delta Wing. Tech. Note No. Aero. 2188, British R.A.E., Sept. 1952.
11. Mayer, John P.: A Limit Pressure Coefficient and an Estimation of Limit Forces on Airfoils at Supersonic Speeds. NACA RM L8F23, 1948.



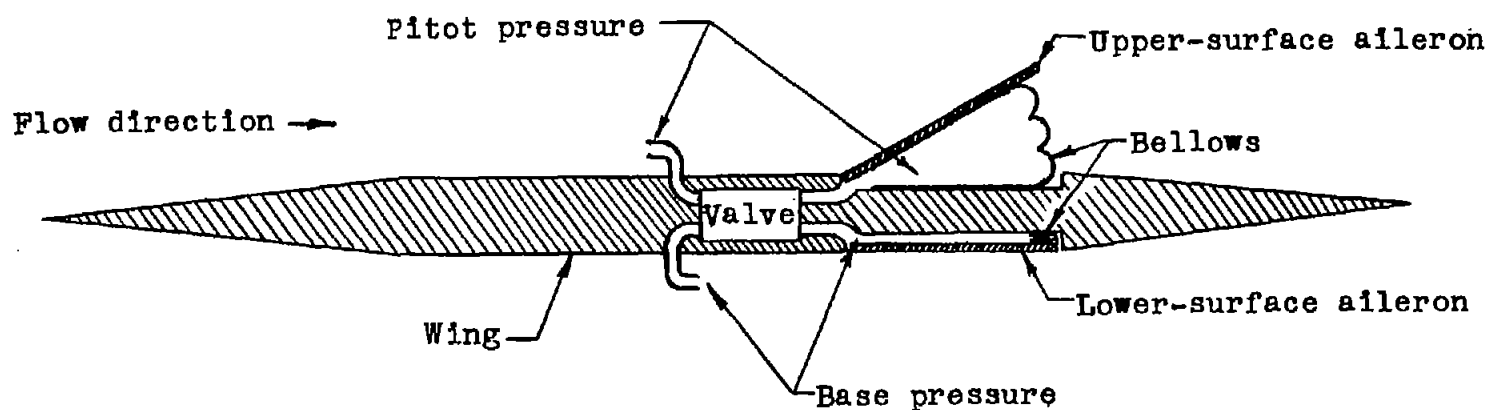
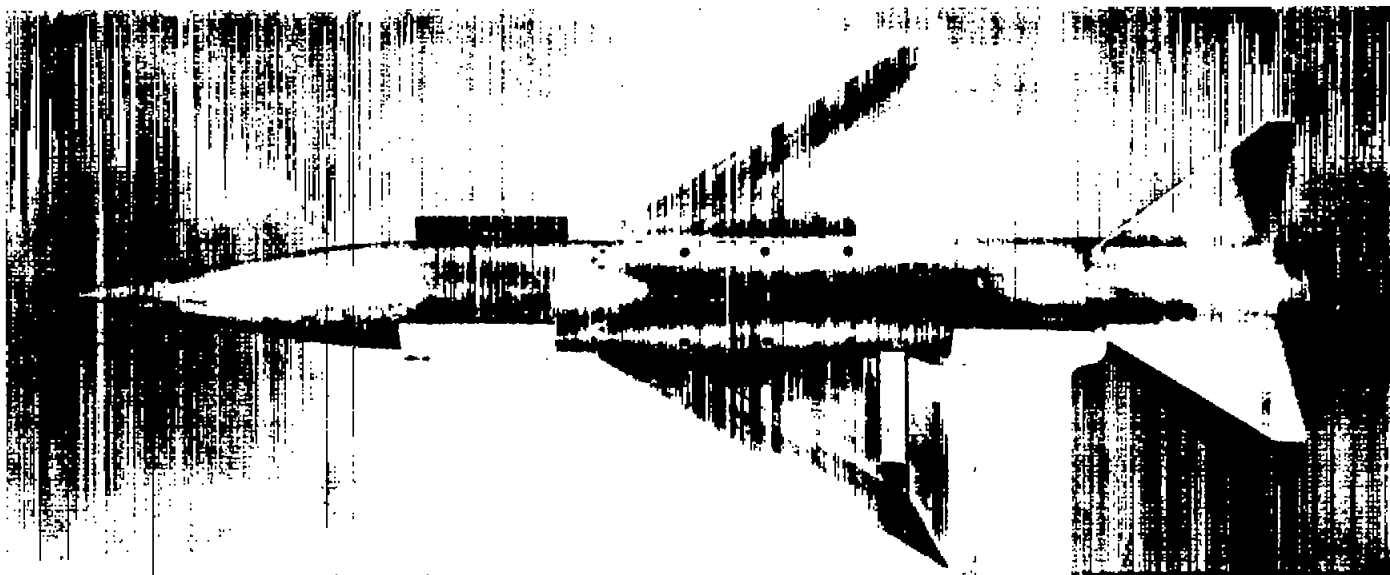
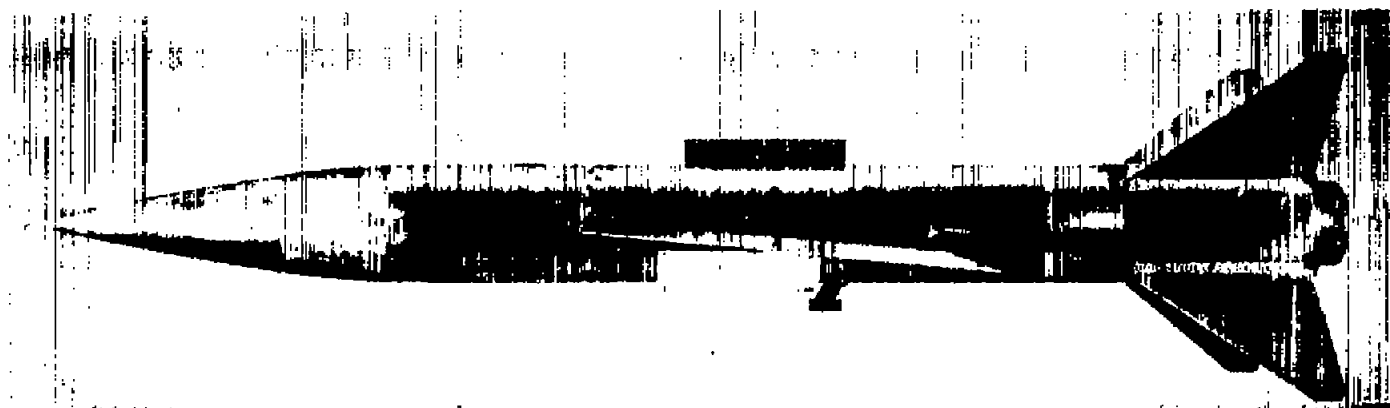


Figure 1.- Schematic sketch of a possible wing-aileron arrangement in which bellows are employed to actuate the ailerons.



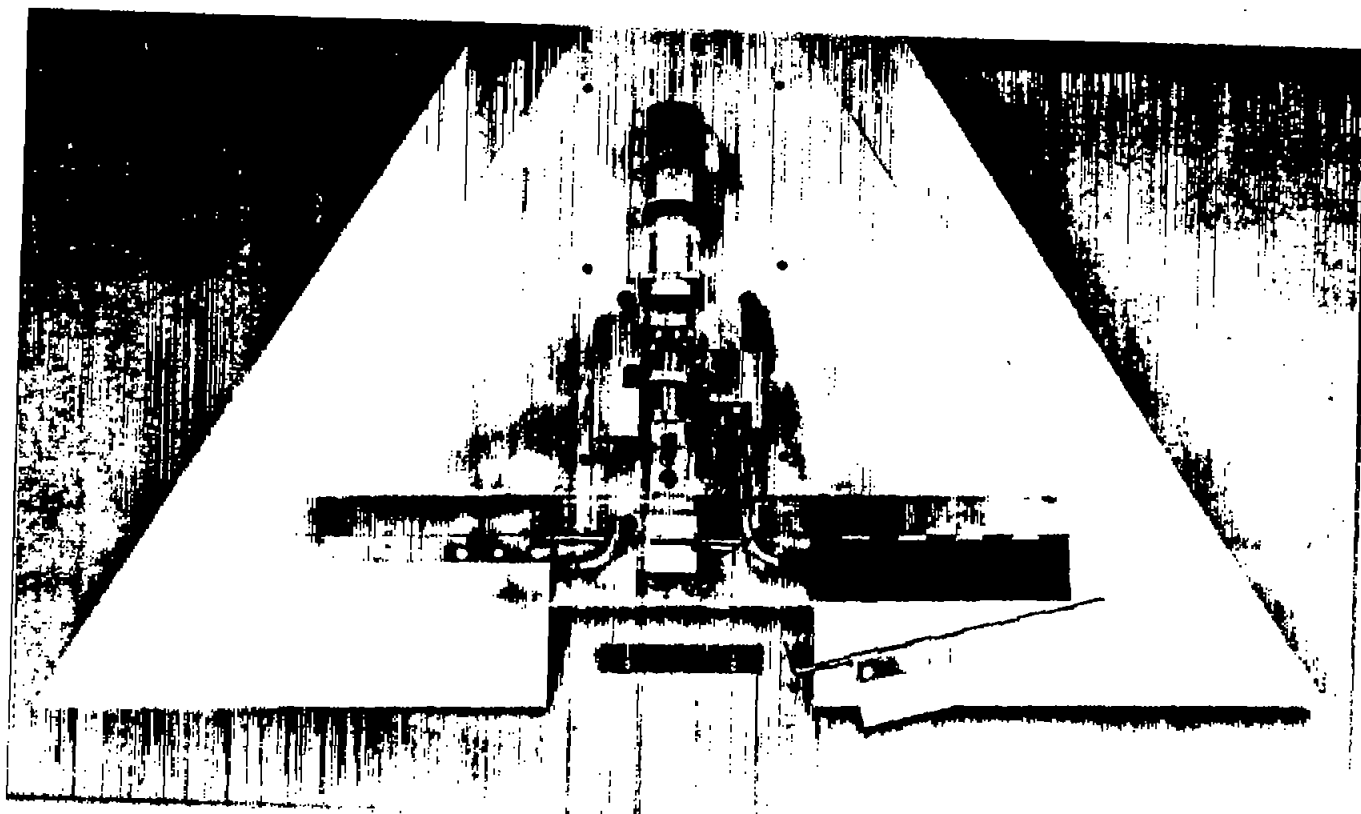
L-80104



L-80102

(a) Model configuration.

Figure 2.- Photographs of configuration used in the present investigation.



(b) Wing configuration disassembled to show control mechanism.

L-79590

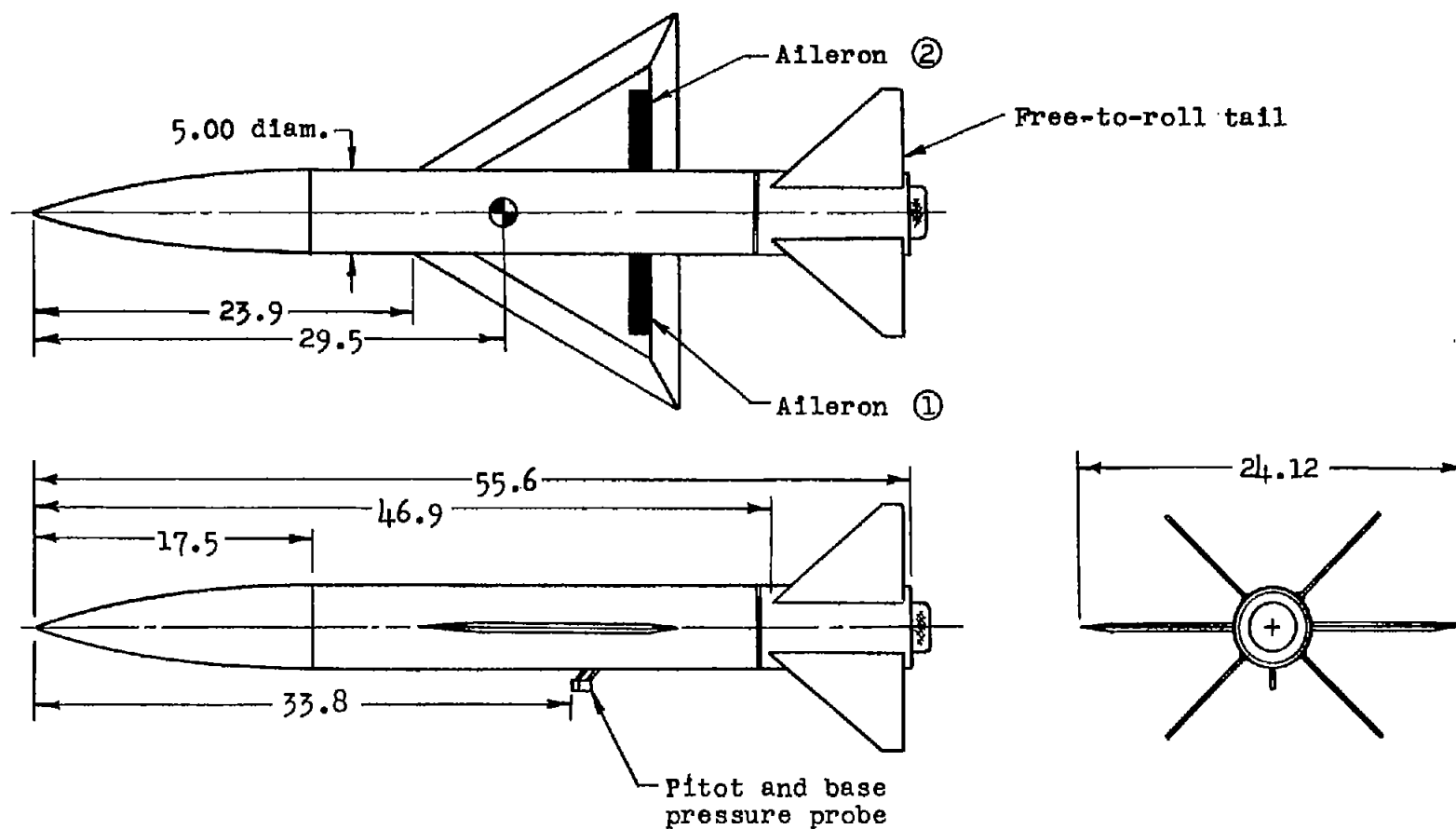
Figure 2.- Continued.



L-80088

(c) Model and booster on launching stand.

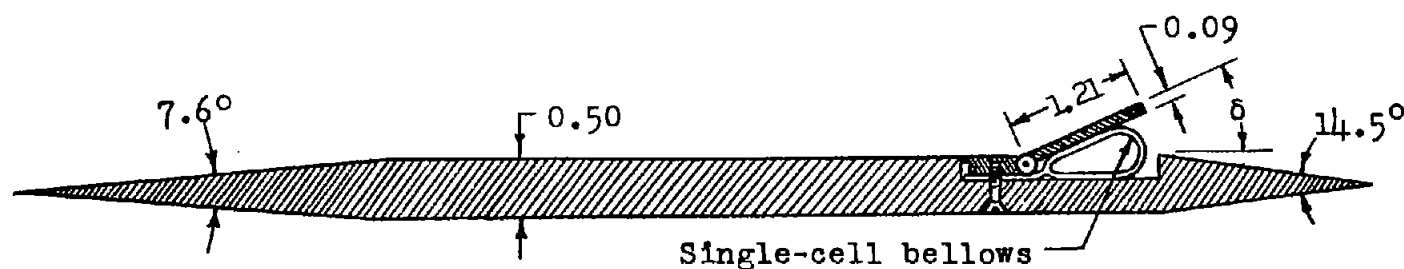
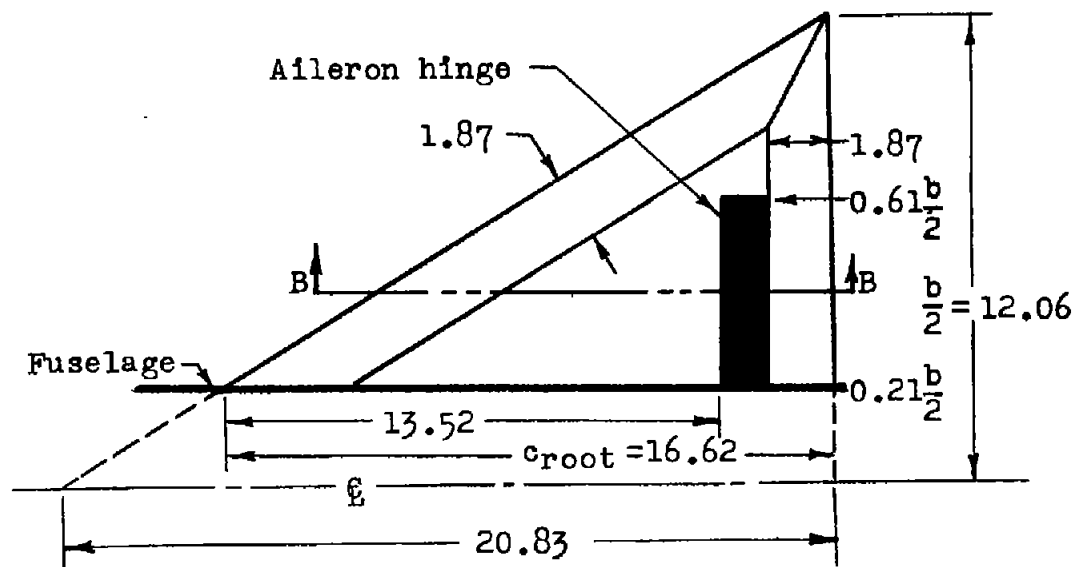
Figure 2.- Concluded.



(a) Test vehicle.

Figure 3.- Geometric details of configuration used in the present investigation. All dimensions are in inches.

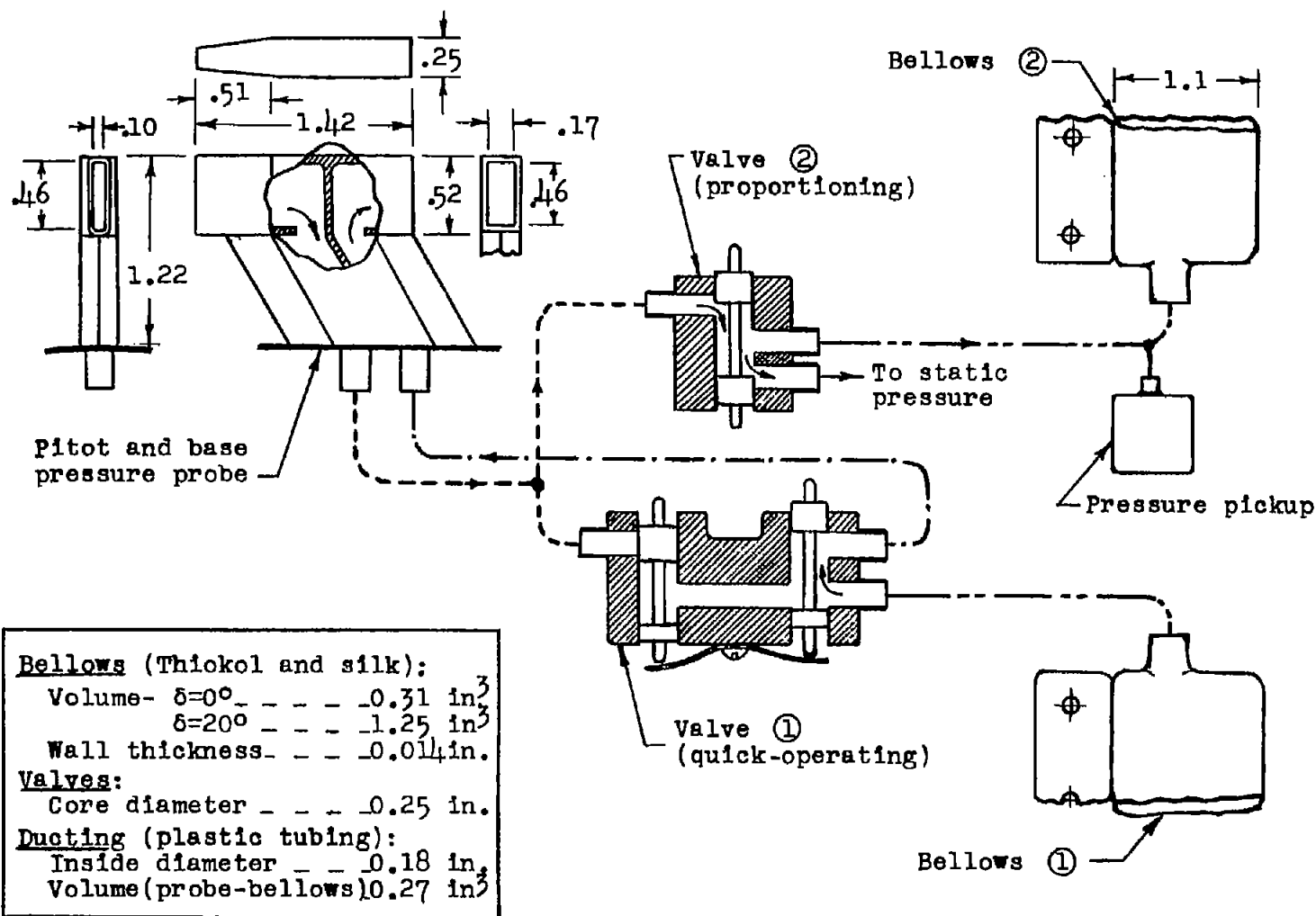
<u>Wing (2LS-T):</u>	
$\Lambda$ - - - -	$60^\circ$
$A$ - - - -	2.31
M.A.C. - -	13.90
<u>Aileron (2LS-T):</u>	
$A_f$ - - - -	4.00
$2y_f/b$ - -	-0.40
$c_f/c_{root}$ -	-0.073
$s_f/s_{exposed}$	-0.037



Section B-B (mid-ailerion)

(b) Wing and aileron arrangement.

Figure 3.- Continued.



(c) Probe, valves, and ducting arrangement.

Figure 3.- Concluded.

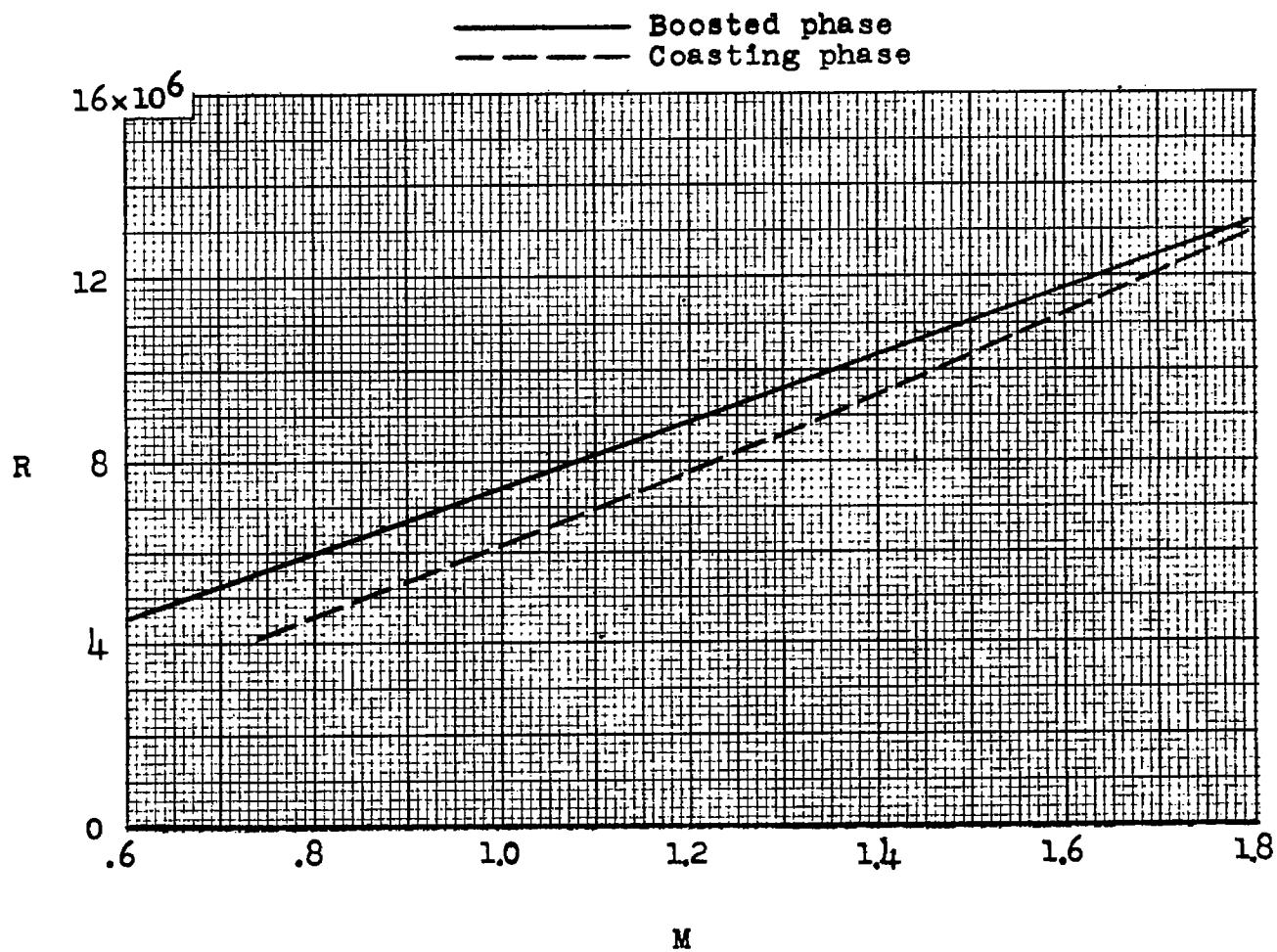


Figure 4.- Variation of test Reynolds number with Mach number; Reynolds number is based on wing mean aerodynamic chord (1.158 ft).



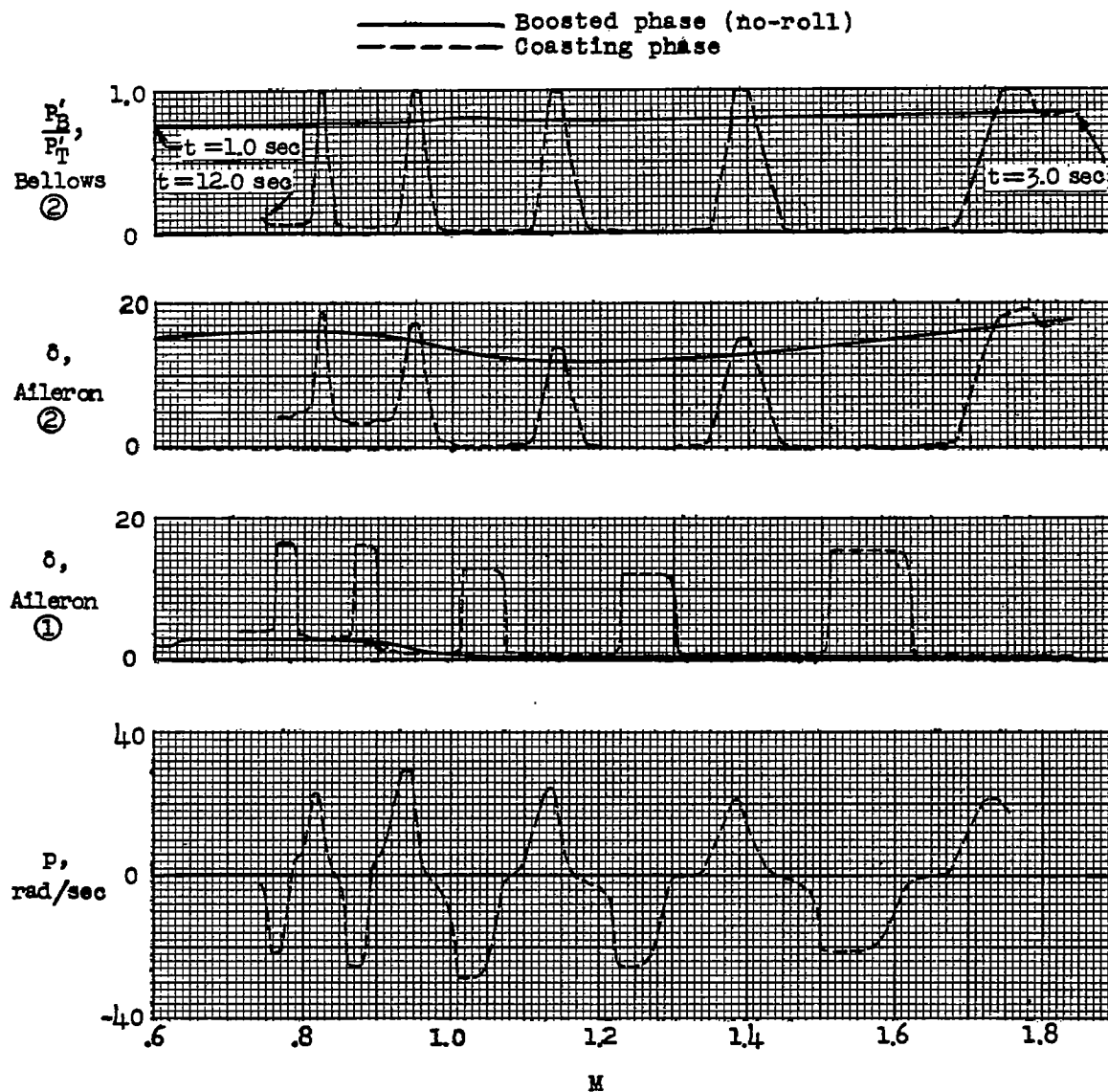


Figure 5.- A flight history, plotted as a function of Mach number, of measured values of bellows pressure in cell ②, aileron deflections, and resulting rolling velocities.

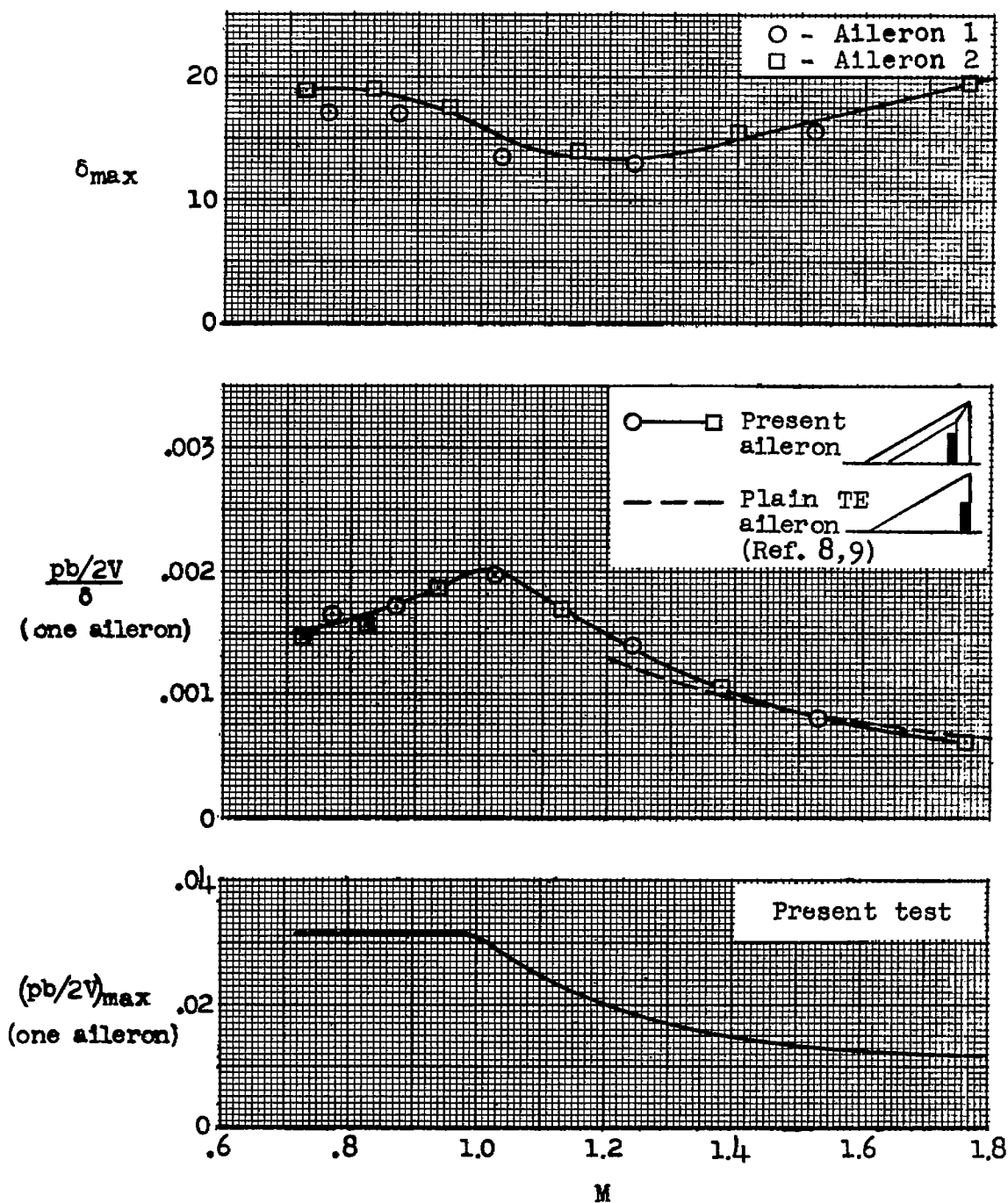
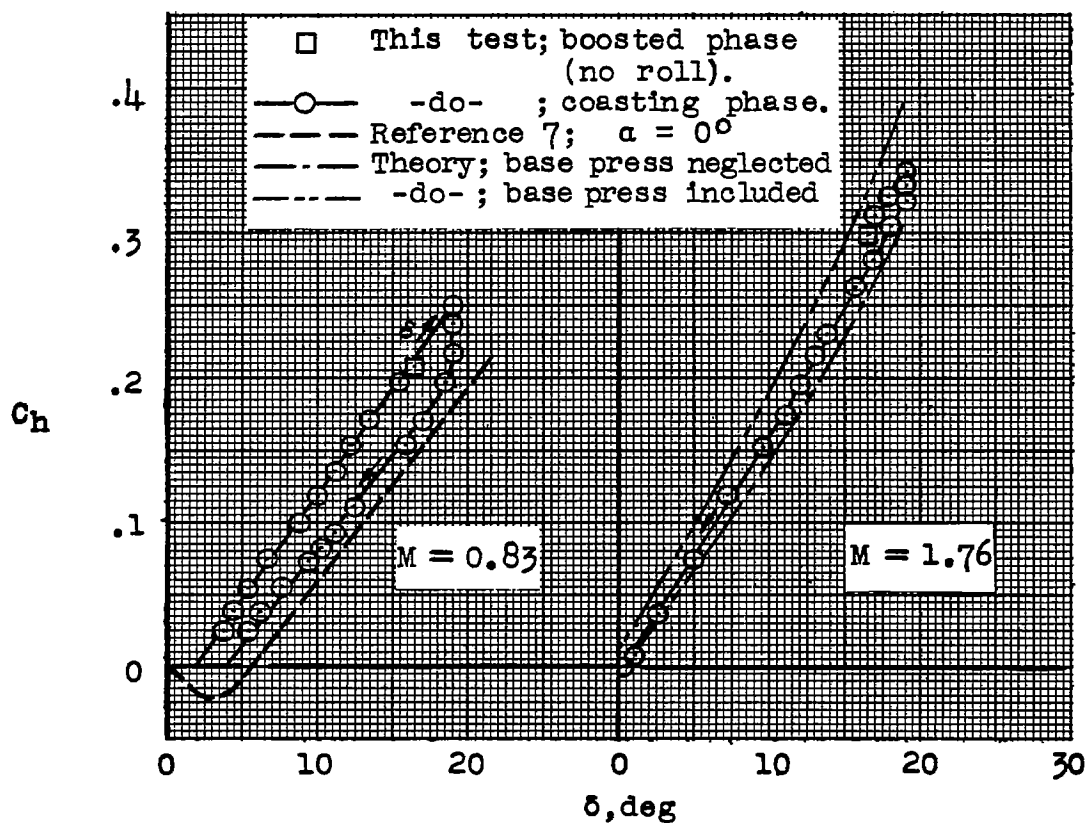
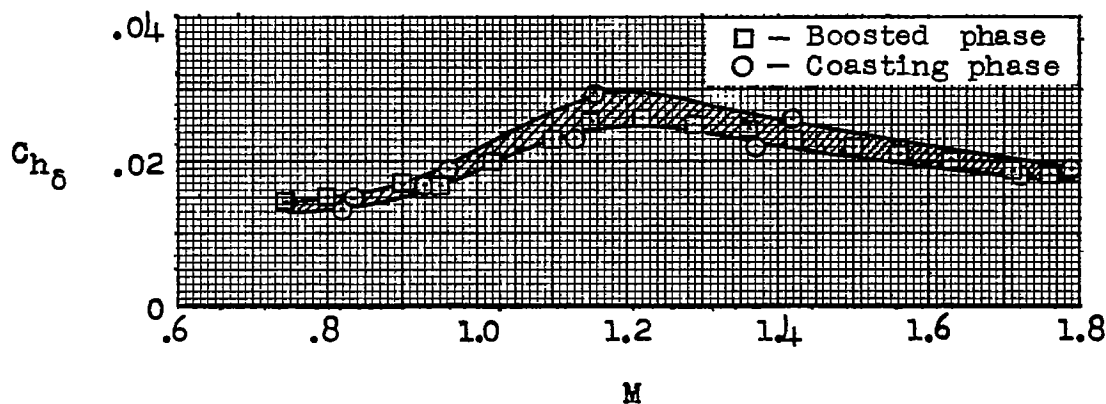


Figure 6.- Variations with Mach number of measured maximum aileron deflection and rolling effectiveness obtained with the bellows-actuated aileron control configuration of the present test, and comparison with other data.



(a) Typical variations with aileron deflection of the hinge-moment coefficient neutralized by the bellows, and comparisons with experimental data from reference 7 and two-dimensional second-order theory.



(b) Variation with Mach number of average slopes of hinge-moment-coefficient curves for the present-test aileron.

Figure 7.- Measured hinge-moment characteristics of the test aileron.

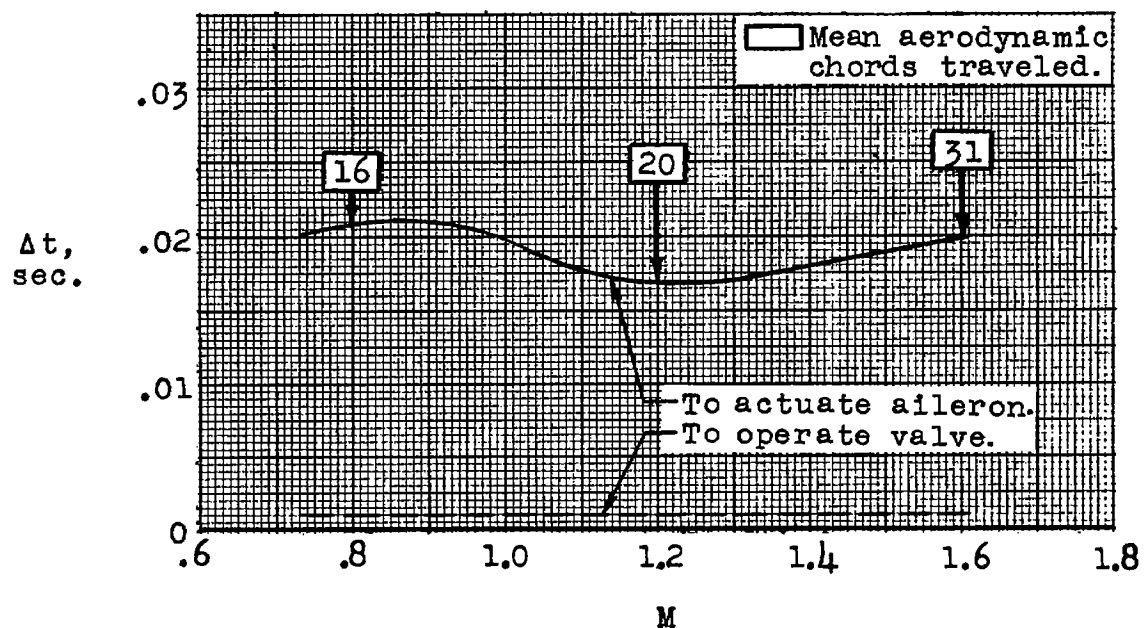
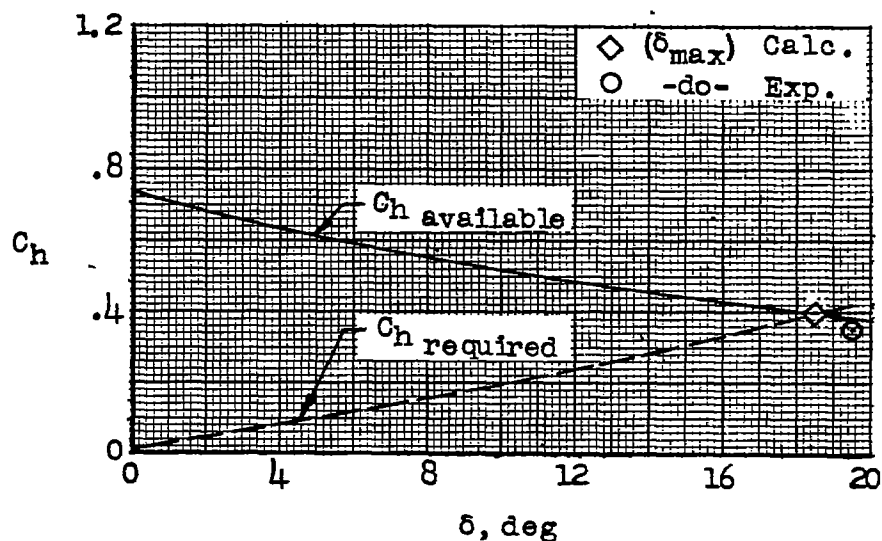
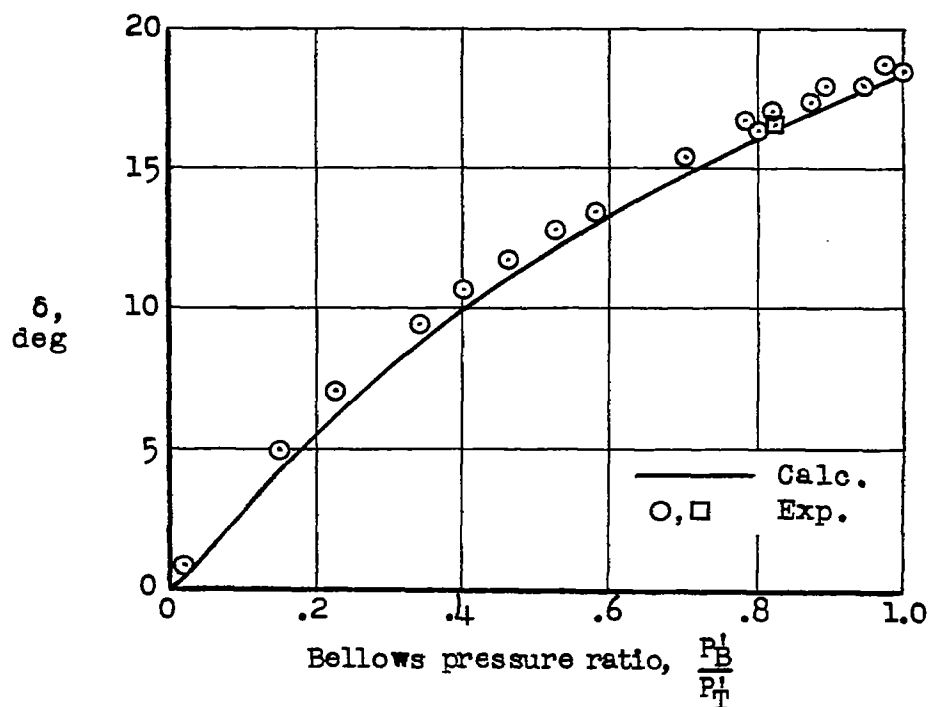


Figure 8.- Variation with Mach number of maximum measured time to deflect or retract aileron and of chord lengths traveled during this interval.



(a) Calculation of the maximum aileron deflection obtained with pitot pressure.



(b) Calculated aileron deflections for bellows pressures less than pitot pressure.

Figure 9.- Comparison of calculated and experimental aileron deflections obtained with bellows pressures up to pitot pressure  $M = 1.76$ ;  $A_F = 4$ ;  $D = 0.1$ .

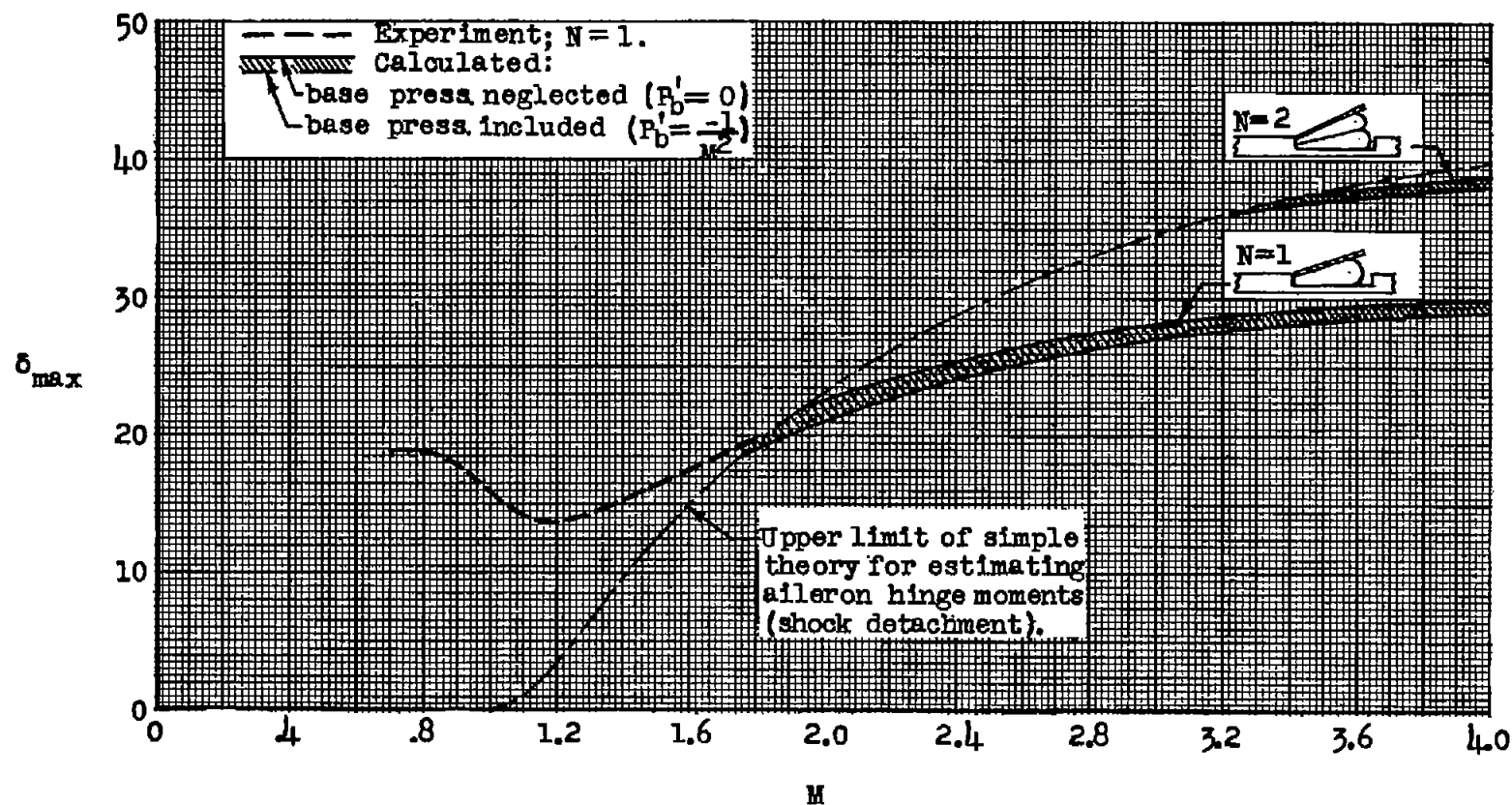
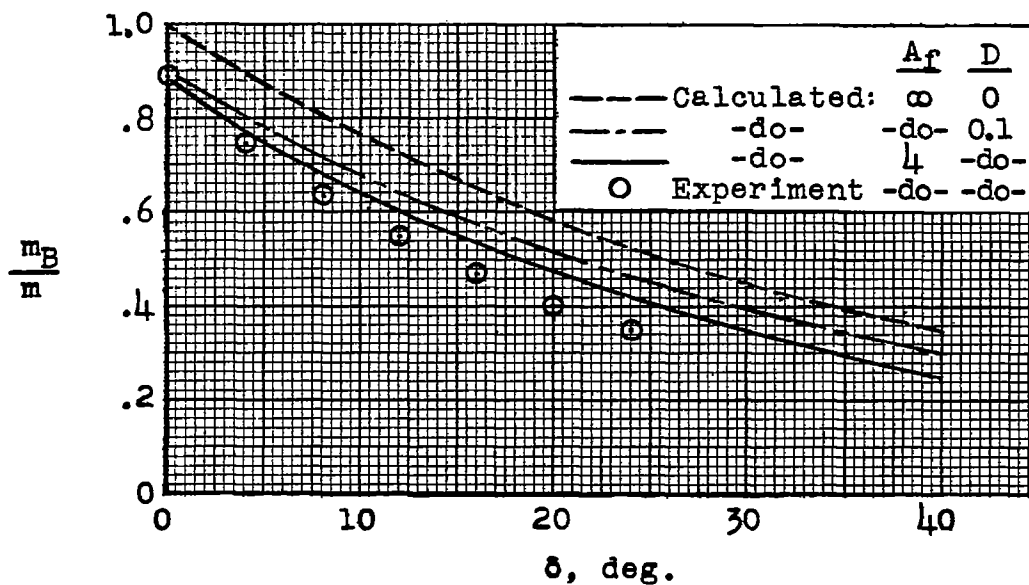
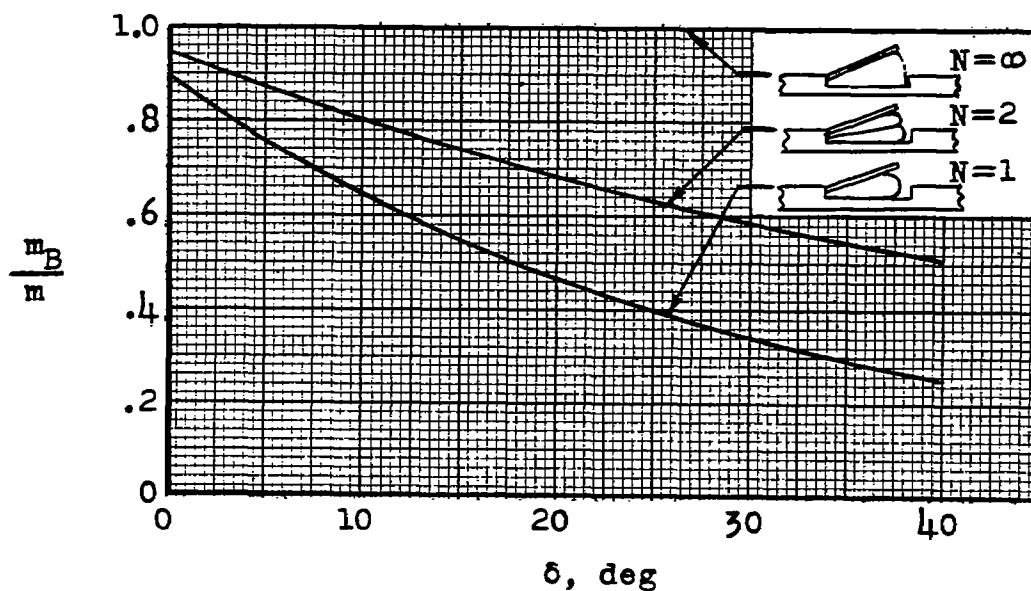


Figure 10.- Variation with Mach number of calculated maximum aileron deflection for a single-cell and a double-cell bellows inflated with pitot pressure  $A_p = 4.0$ ;  $D = 0.1$ .

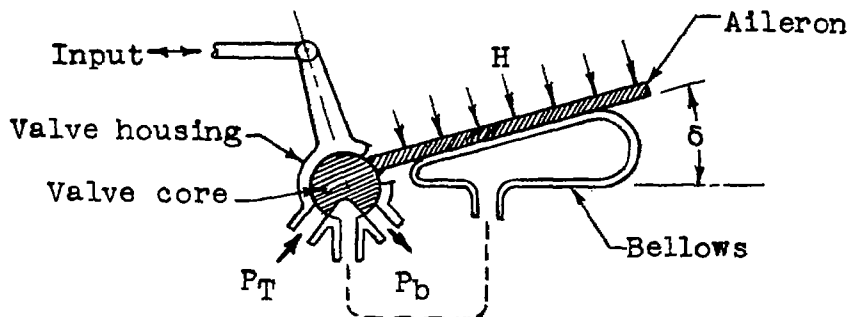


(a) Variation with aileron deflection of calculated and experimentally derived values of bellows effectiveness parameter  $N = 1$ .

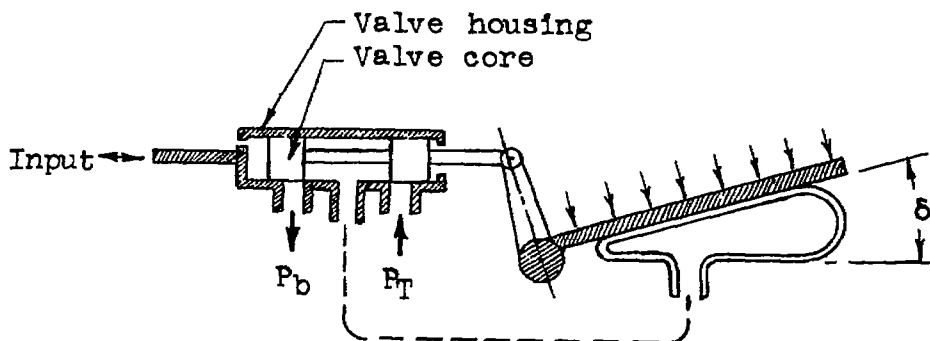


(b) Effect of number of bellows cells on calculated bellows effectiveness parameter  $A_f = 4$ ;  $D = 0.1$ .

Figure 11.- Variations with aileron deflection of the bellows moment-area ratio or effectiveness parameter.



(a) Control employing rotary-type valve.



(b) Control employing lineal-type valve.

Figure 12.- Two variations of an aileron-deflection control employing feedback.



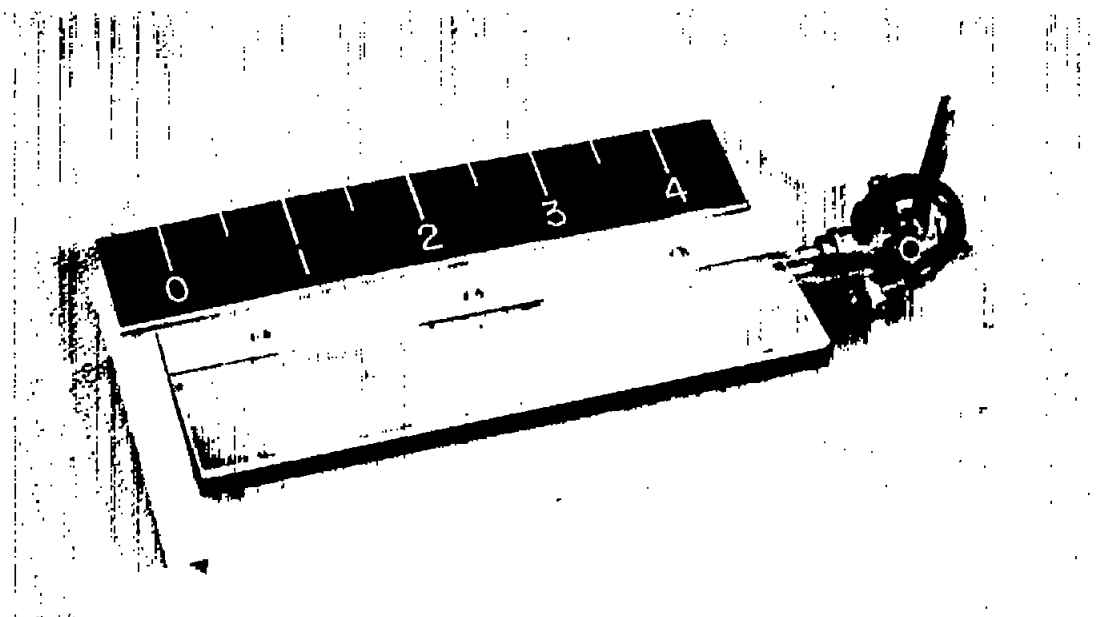


Figure 13.- Mock-up of bellows-actuated aileron with deflection control employing mechanical feedback. Aileron plan form and bellows are identical to those in flight-test model.

L-81156

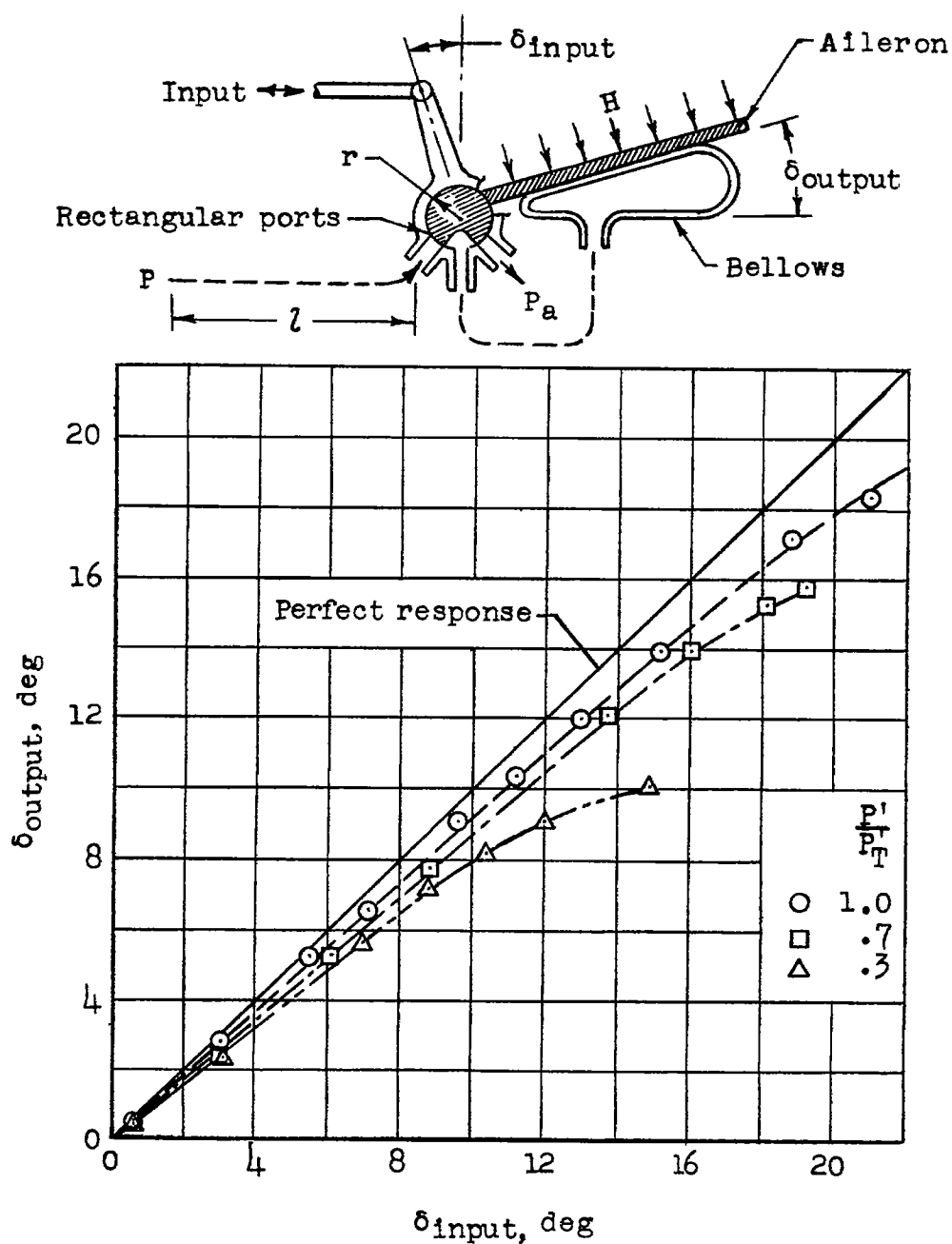
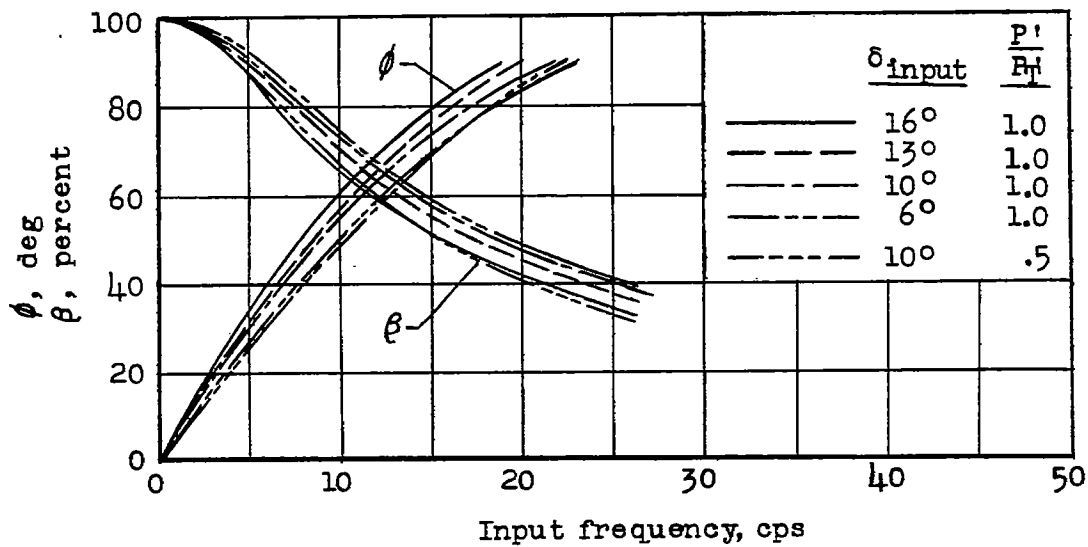
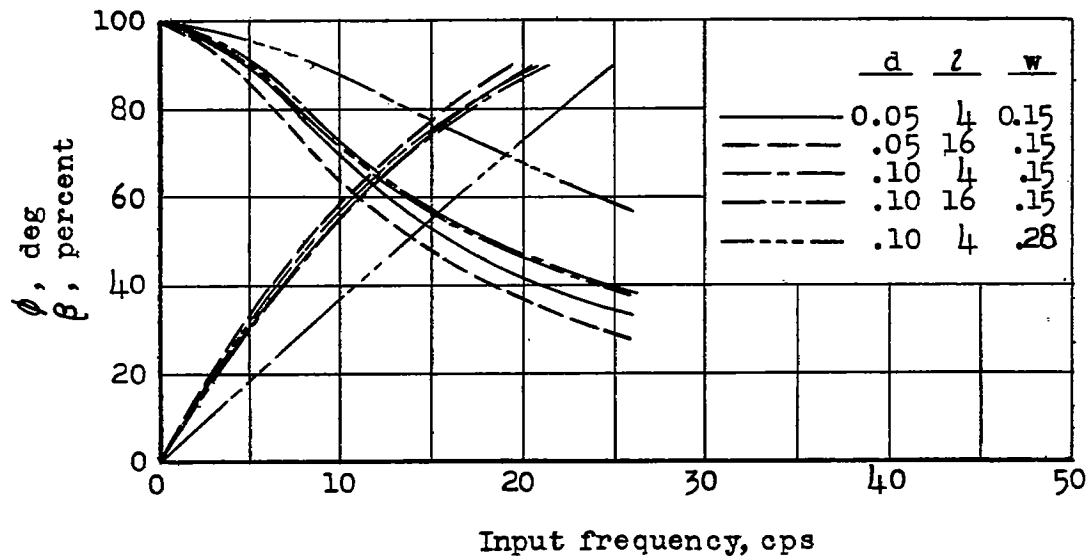


Figure 14.- Static response characteristics of an aileron-deflection control with feedback. Aileron loading  $H/\delta$  and pitot pressure  $P_T$  are simulated for  $M = 1.9$  at sea level,  $r = 0.1$ ;  $w = 0.15$ ;  $A_F = 4$ ;  $D = 0.1$ .



(a) Some effects of variations in input amplitude  $\delta_{input}$  and inlet pressure ratio  $P'/P'_T$  on the phase-lag angle and output amplitude ratio.  $d = 0.1$ ;  $l = 4$ ;  $w = 0.15$ .



(b) Some effects of changes in duct and valve-port geometry on the phase-lag angle and output amplitude ratio.  $\delta_{input} = 10^\circ$ ;  $P'/P'_T = 1.0$ .

Figure 15.- Frequency-response characteristics of a bellows-actuated aileron-deflection control with feedback. Aileron loading and pitot pressure simulated for  $M = 1.9$  at sea level,  $r = 0.1$ ;  $A_T = 4$ ;  $D = 0.1$ .